

# AAR IN FURNAS DAM, BRAZIL, RESIDUAL EXPANSION AND THE EFFECT OF LITHIUM

Nicole P. Hasparyk<sup>1,\*</sup>, Paulo J. M. Monteiro<sup>2</sup>, Denise C.C. Dal Molin<sup>3</sup>

<sup>1</sup>PhD., FURNAS Centrais Elétricas S.A., Concrete Laboratory,  
Department of Support and Technical Control, GOIÂNIA, Brazil

<sup>2</sup>PhD., University of California, BERKELEY, United States of America

<sup>3</sup>PhD., Federal University of Rio Grande do Sul, UFRGS, NORIE, PORTO ALEGRE, Brazil

## Abstract

Furnas Hydraulic Power Plant is located in Brazil, and it was built in 1963. The occurrence of the AAR in the concrete of Furnas was first noticed in 1976. Once the AAR was recorded, the structure was monitored by instruments and concrete cores were studied in the laboratory through several tests and microscopy analyses.

We report an experimental program involving concrete cores from the spillway driftway (both upstream and downstream) of Furnas Dam. Visual inspection and microscope analyses were performed to identify the reactive aggregates and expansive products of AAR. The expansion tests exposed the concrete cores to three different immersed conditions: in water, in NaOH solution and in a lithium nitrate/sodium hydroxide solution (0.74M) at 38°C. The results confirmed the AAR, the presence of residual expansions in the concrete cores and the potential of using lithium nitrate as admixture to minimize the ASR expansion.

**KEYWORDS:** AAR, expansion testing, lithium, microscopic analyses, concrete microstructure

## 1 INTRODUCTION

Alkali-aggregate reaction (AAR) has caused degradation to several structures such as dams, bridges and marine structures. In some cases, and mainly in structures with hydrodynamic and electric equipments, the costs of maintenance and rehabilitation are quite high. Although this phenomenon was discovered over sixty years ago [1], there is still great difficulty in controlling the deleterious effect of AAR once it develops in a concrete structure. The long-term monitoring of the displacements and cracks in a structure affected by AAR helps the assessment of its life-prediction. Even so, a complete investigation involving the drilling of cores is sometimes necessary to make a realistic diagnosis of the structure and to determine the degree of AAR deterioration.

Furnas Dam is a Hydroelectric Power Plant (HPP) in Brazil (Figure 1a) that manifested the symptoms of AAR. This reaction was first reported in 1976. The greatest concerns were the appearance of cracks in the top of the spillway columns, in the anchorage blocks of the water conduits, and in the powerhouse. Also an unleveling between the central wall and adjacent blocks was observed. Once AAR was reported, the concrete structures were monitored by instruments, and concrete cores (Figure 1b) were studied in the laboratory through several tests and microscopy analyses. Figure 2a shows the main occurrences of cracks due to AAR in a column of the spillway, and Figure 2b shows an exuded ASR gel in the concrete of the spillway. This paper presents part of the studies performed with aggregates and concrete cores from Furnas HPP.

## 2 EXPERIMENTAL PROGRAM

### 2.1 Samples and tested concretes

The experimental program was divided in two parts: a) aggregate tests were performed in order to determine its reactivity and b) concrete samples were drilled and several tests were performed.

The aggregate studied in the first part of the program was collected in a deposit next to Furnas power plant in the 90s, being probably a similar nature of rock used in concretes. The aggregate from drilled concretes was also studied for comparison. Concrete samples were drilled from the driftway of

---

\* Correspondence to: [concreto@furnas.com.br](mailto:concreto@furnas.com.br)

the spillway of Furnas HPP in both directions, upstream and downstream. The cylindrical concrete cores were approximately 15 cm in diameter by 30 cm in length.

The driftway, built in 1961, is made up of six bands of concrete blocks, 14.5 m each (related to six spillways) and two blocks 8.75 m each (left and right abutments), adding up to a 104.5 m driftway. These blocks were built in 13 layers, about 1.5 m height each. In order to evaluate the same type of concrete, layer number 7 in the driftway was selected for this study and represents a 45 years old concrete. Its mixture proportion contained 170 kg/m<sup>3</sup> of cement, 550 kg/m<sup>3</sup> of sand (natural and artificial), 1590 kg/m<sup>3</sup> of crushed rock (maximum size of 152 mm) and 0.70 water-cement ratio. In the concrete both natural and artificial sand of quartzite from the excavations and an Ordinary Portland cement manufactured nearby Furnas dam were used, with no mineral admixture, having a total maximum alkalis of 0.60% according to the standard recommendations at that time.

It is important to point out that during the visual investigation, different stages of AAR were observed and therefore, three concrete classes were defined: downstream (DS), upstream 1 (US1), and upstream (US2). The concrete in downstream direction was considered unaltered (DS Class), as it did not present superficial signs of deterioration during visual inspection. The upstream direction was divided into 2 classes (US1 and US2), both affected by ASR. Concrete in Class US1 had less damage, as evidenced by a lower incidence of characteristics relating to AAR (designated less affected concrete), while Class US2 showed greater damage (designated more affected concrete).

## 2.2 Test methods

### *Study of aggregates*

Aggregates collected near Furnas Dam and also aggregates from concrete cores were analyzed according to ASMT C-295 [2] in polished thin sections and billets to identify their mineralogical characteristics using both transmitted and reflected light optical microscope, respectively. Expansion tests according to accelerated mortar bar test of ASTM C-1260 [3] were also performed with the aggregates obtained from the quarry to investigate its potential reactivity. Concrete prisms were also tested according to ASTM C-1293 [4]. An Ordinary Portland cement from Brazil (Goias State) with the following oxide composition was used: SiO<sub>2</sub> 20.75wt%, CaO 64.65wt%, Al<sub>2</sub>O<sub>3</sub> 4.52wt%, Fe<sub>2</sub>O<sub>3</sub> 2.56wt%, MgO 1.16wt%, SO<sub>3</sub> 2.44wt%, with 1.32wt% and 0.83wt% total and soluble alkali, respectively. In the concrete tests, natural non-reactive sand of quartz was used (the expansions made with this sand were less than 0.10% in the accelerated mortar bar test and equal to 0.07% at 16 days).

### *Core assessment: a) visual inspection*

Cores drilled from the driftway were classified by visual inspection. Within each class (US, DS1 and DS2) all the samples were inspected visually and with magnifying glass to record the presence of any possible characteristics (symptoms) related to AAR, according also to some parameters of ASTM C-856 [5], such as:

- Voids filled with material
- Cracks (in the mortar or in the aggregates)
- Reaction rims
- Dark stains in the mortar or around the aggregates
- Detachments

### *Core assessment: b) microscopic analyses*

Analyses using scanning electron microscope (Leica, S440i) were performed in six concrete cores (two cores for each class: US, DS1 and DS2). From each class two cores were selected: one with the least (LI) and the other with the greatest (MI) amount of deterioration. Internal portions of broken samples in fracture surface selected from each concrete core were analyzed using secondary electron (SE), and X ray dispersive energy spectrometry (EDS), just for a qualitative analysis. Samples were sputtered with gold to become conductive and the operating conditions were set at 20kV and 1nA, at high vacuum ( $5 \times 10^{-5}$  Torr).

### *Core assessment: c) expansion testing*

In order to perform expansion tests, concrete cores were cut to obtain 285-mm long cylinder and stainless studs were inserted in the center core extremities to allow the recordings of length changes. Twenty eight concrete cores were tested for the following classes: downstream (DS), upstream 1 (US1), and upstream 2 (US2).

The expansion tests were performed under the following conditions: submerged in water; submerged in NaOH solution and submerged in a lithium nitrate : sodium hydroxide solution at a

molar concentration of 0.74. All samples were kept at 38°C temperature and length readings were made up to 365 days. Four concrete core samples were tested for each class (DS, US1 and US2) in the first two exposure conditions and 4 samples in the last condition, in this case from upstream 1 (US1).

### 3 EXPERIMENTAL RESULTS

#### 3.1 Petrography and expansion testing of aggregate

Both aggregates, from the quarry and from the concrete cores, presented similar features being classified as quartzite, containing similar mineralogical composition as determined by optical microscopy with transmitted light: quartz: 85 to 90vol%; muscovite: 5 to 10vol%; opaque minerals: < 5vol%. The samples showed fine granulation, granoblastic texture and strong metamorphic foliation, which is determined by preferred orientation of the laminar flakes of muscovite and by the elongated strained quartz with sutured boundaries between adjacent quartz grains. Quartz crystallites often show undulatory extinction due to strain, but euhedral quartz grains do not occur. Muscovite occur as small oriented flakes interspersed between quartz grains. Opaque minerals occurred disseminated throughout the rock, but preferentially around the micaceous minerals. Mineralogical composition associated with texture indicates that this rock consists of metamorphosed arenitic sediments. Figures 3 and 4 present micrographs of the main features of quartzite samples in the optical microscope at 40× magnification.

In order to investigate mineral constituents of opaque zone such as iron sulphides, an analysis was performed with reflected light microscope. In the aggregates from the quarry, pyrite, hematite and limonite were present. Pyrite occurred as subeuhedral crystals with some of them showing alteration for limonite. However, the aggregates from the concrete cores did not have sulphides and the opaque zone was identified as hematite.

Figure 5 shows the average expansive behavior of the mortar bars (mb) and concrete prisms (cp) cast with quartzite according to ASTM C-1260 and ASTM C-1293, respectively. The average expansion in the mortar bar tests was higher than the threshold of 0.20%  $\ell/\ell$  at 16 days. The average expansion was 0.24%  $\ell/\ell$  and 0.39%  $\ell/\ell$  at 16 and 30 days, respectively. Similarly, the concrete prisms expansion tests gave values that were higher than limit of 0.04%  $\ell/\ell$  even at 155 days. At one year, average expansion was 0.09%  $\ell/\ell$ .

#### 3.2 Petrography and expansion testing of concrete

##### *Visual inspection*

Figures 6 to 9 present some images from the visual inspection indicating the presence of reaction products typical of AAR.

##### *Microscope analyses*

SEM analysis of sample LI from downstream class showed little evidence of ASR products with the exception in a zone that visually was darker than the rest of the cement paste, where a massive phase typical of gel was observed. In the sample MI, where AAR was most prevalent, the interfaces between the cement paste and the aggregates were well preserved, however cracked gel with botryoidal aspect was observed in the darker zones. Also crystallized products with silico-alkaline composition were formed on the aggregate (see Figures 10 and 11).

In sample LI from upstream class 1 (US1), alkaline crystallized products were observed inside the voids whereas massive and cracked gel were found in the dark zones of the mortar and fine crystals around the aggregate interface. In sample DS-MI, the investigation identified cracked gel around the voids (associated to the vitreous rims in the voids by visual observation), crystallized products of AAR in voids (white material visually) and some ettringite in the matrix. Figures 12 and 13 show the products from US1 class.

In the sample LI (belonging to class US2), SEM observations showed voids filled with crystallized products with silico-alkaline composition, massive and cracked gel and fine crystals, some of them ettringite, in the mortar. The sample had the following DS-MI characteristics: fine crystals in the interfacial transition zone (the rims observed in the visual inspection) and in the aggregate, several products such as massive gel and crystallized phases in laced crystals in the voids, alkali-calcium-silica crystals in mortar and ettringite. Micrographs 14 and 15 shows some of the phases of AAR observed in class US2.

##### *Expansion tests*

The average residual expansion over time for the four core samples of each class (DS, US1 and US2) immersed in water at 38°C are shown in Figure 16. The experimental results of the concrete

cores tested in this condition were best fit according to the following equation  $y = a(1 - \exp^{-b \cdot x})$ . The average residual expansion over time for the four core samples of each class (DS, US1 and US2) submerged in NaOH (1N) at 38°C and the results for the cores from US1 class tested in a lithium nitrate:sodium hydroxide solution at a molar concentration of 0.74 are given in Figure 17. In those exposure conditions, the experimental results of concrete cores tested were best fit according to the equation  $y = 1 / (a + b \cdot x^c)$ .

#### 4 DISCUSSION

The mineralogical study of quartzite indicates that the main reactive constituent is strained quartz [6-10,12]. The presence of strained elongated quartz grains indicates that the rock was exposed mainly to shearing strain [10]. In addition, the fine size of the quartz crystallites intensifies the area for dissolution of silica from quartzite [11].

It is important to point out that the measurement of the undulatory extinction angle by optical microscopy of quartz grains is a limited method for the definition of the deformation degree of the rock. When a rock undergoes severe deformation during metamorphism, the undulatory extinction angle can disappear, resulting in false results. Another method that can study different degrees of rock deformation is texture analysis, and preferred orientation of micaceous minerals that is responsible for rock foliation is the main factor related to rock reactivity [13]. In relation to sulphides present in opaque minerals, it is known that they can oxidate and produce an internal source of sulfate and deteriorate concrete, depending on its intensity and exposure conditions [14,15]. In the quartzite samples, pyrite crystals were present in minor amounts. Since this subject is not the main focus of this study, it will not be further discussed here.

Visual characteristics of AAR were observed in almost all concrete cores and with greater intensity in the cores from US1 and US2. DS class presented symptoms of deterioration, but with minor incidence.

SEM analyses confirmed the presence of alkali-aggregate reaction in almost all samples of concrete cores. A qualitative analysis indicates that the cores from downstream class (DS) had a lower incidence of AAR products in comparison to the cores from upstream class (US1 and US2). US2 class presented the greatest incidence of reactive phases from AAR. All the reaction products contained mainly silicon, potassium and calcium with varied morphologies of AAR crystallized products and gel [12,16].

Accelerated mortar bar expansion tests and also concrete prism tests indicate the deleterious behavior of quartzite due to expansions higher than thresholds of both methods. Expansion tests of concrete cores immersed in water (Figure 16) showed an expressive increase in expansion at early ages and in general up to 28 days. After that, it was not noticed an increase of expansions. At 365 days, the largest expansion was 0.11%  $\ell/\ell$  for one sample from US1 class. The average expansion was about 0.08%  $\ell/\ell$ . With the purpose to verify statistically the influence of concrete class (DS, US1 and US2) on the expansions, a variance analysis was performed considering individual data at 180 and 365 days [17]. Nevertheless, the results indicate that there are not significant differences between the three classes for a significance level of 0.05% in the exposure condition tested from this analysis.

Hasparyk et al. [18] reported expansions from 0.02%  $\ell/\ell$  to 0.06%  $\ell/\ell$  at one year in concrete cores exposed to 100% RH at 38°C from different structures of hydraulic power plants. It is known that water plays an important role in chemical reactions. According to Poole [19], water has two functions, the first allows migration and movement of alkaline cations and hydroxyl ions, and the second function is related to gel adsorption leading to expansions. When a concrete is deteriorated by AAR, it contains gel in its interior in a non saturated form. Any additional water can produce expansion due to gel adsorption [19,20]. This behavior can explain the high values of expansion detected at first ages in the present study. Thus, the occurrence of high expansions at first ages cannot be linked only to the saturation of concrete by water absorption but also to the adsorption of pre-existent gel followed by its expansion. On the other hand, expansions that are detected at more advanced ages can be related to new formed gel and its water adsorption.

Figure 17 shows an expressive increase in expansion up to 28 days followed by a constant period at around 90 days for concrete samples in DS class and 112 days for US1 and US2 classes that were immersed in NaOH. After that, expansions do not stop and it is verified a gradual but expressive increase of expansion over time for US1 and US2 classes, and less intensive for DS class up to one year. The largest expansion value measured was 0.18% at one year for US2 class. The average expansions at this age were 0.09%, 0.14% and 0.15% for DS, US1 and US2, respectively. The smaller expansion observed in class DS suggests a reduced pre-existing gel when compared to other classes. On the other hand, reactive aggregate tends to be higher and can lead to higher expansions in a high

alkaline environment. However, micro-cracking due to AAR observed in the DS cores is smaller than in the US1 and US2 classes, thus a smaller level of cracking can difficult the entrance of alkaline hydroxides from solution to interior of concrete resulting in smaller expansion.

Grattan-Bellew and Danay [21] observed high expansions in concrete cores deteriorated by AAR (about 0.25%  $\ell/\ell$  after one year) when immersed in NaOH solution at 38°C. From others [18], the measured expansion was lower, varying from 0.05%  $\ell/\ell$  and 0.08%  $\ell/\ell$  and ceasing in majority after 190 days.

With the purpose of verifying statistically the influence of the concrete class (DS, US1 and US2) on the expansion at exposure condition of immersion in NaOH at 38°C, a variance analysis was also performed at 180 and 365 days individually [17]. Results indicate that there are significant differences between the three classes for a significance level of 0.05% for this the exposure condition. In addition, the Duncan's multiple range test of homogeneity of groups [22] was performed for each age mentioned above. This method was used to determine a range statistic for each comparison by ordering the group means from smallest to largest and the number of steps that two means are apart in the ranking. The results indicate that US1 and US2 class are statistically similar while DS class formed a different group.

By immersing the samples in NaOH, the reaction products have water to expand and the alkaline hydroxides can generate new reaction products further increasing the expansion as compared to the immersion in water. The high values of expansion (in the range of 0.09% to 0.15% from cores from three classes) indicate the presence of reactive minerals in aggregates. However, DS class showed a distinct behavior from the others that can be explained by the minor incidence of gel and micro-cracking observed by visual and microscopic analyses.

The tests with cores immersed in Li:Na solution (Figure 17) also showed an increase of expansions at early ages up to 28 days. After that, it was observed a slower increase in expansion, different from the behavior occurred during NaOH immersion. Nevertheless, the reduction of the expansion was not so high. The work done by Folliard et al. [23] on the optimum concentration of lithium indicates that it can depend on aggregate type, minerals and exposure conditions. Thus, despite reducing expansion in the presence of lithium, the employed dosage may not have been the optimum. It is necessary additional studies with materials employed, and also from the geochemical and mineralogical point of view in order to understand the real reasons for this behavior and to verify the optimum concentration. Work by Kaneyoshi et al. [24] using accelerated tests in concrete cores drilled from a column of a bridge showed a reduction in expansions of more than 50%, if an adequate lithium concentration is applied.

#### 4 CONCLUSIONS

Quartzite from Furnas HPP is an aggregate with great potential to develop ASR, causing high expansions as confirmed by both accelerated mortar bar and concrete prism tests. Additionally, visual and microscopic analyses performed on concrete cores showed the presence of expansive products. Downstream concrete showed less deteriorated whereas upstream concrete had more expressive characteristics of the reaction.

Residual expansion tests performed with concrete cores showed promise. Nevertheless, it is important to point out that there are difficulties in the measurements since it is an adaptation of the concrete prism test involving preparation of samples, fixing of studs, testing and readings.

Concrete expansion tests in the cores indicate the presence of minerals in the aggregate with potential to react and maintain expansion. Concrete cores immersed in water expand during the early ages, but there is a tendency of stabilization along time. On the other hand, in NaOH immersion the expansions did not stop and reached up to 0.18% at one year. In this condition, downstream concrete showed smaller expansion (about 0.09%) when compared to upstream concrete cores (0.15% in average). Variation in the intensity of expansions occurred due to availability of water, alkalinity of solution, reactive minerals and pre-existing gel.

In the study with lithium, concrete cores from upstream showed smaller expansions compared to the ones without lithium, however the reduction was just about 24%. This result confirmed the potential of lithium in reducing expansions due to AAR, nevertheless additional tests are necessary and must be accomplished in order to corroborate its efficiency and seek for a better performance.

## 5 REFERENCES

---

- [1] Stanton, TE (1940): Expansion of concrete through reaction between cement and aggregate. In: Proceedings of American Society of Civil Engineers (66): 1781-1811.
- [2] ASTM C295 (2003): Standard guide for petrographic examination of aggregates for concrete. American Society for Testing & Materials, ASTM International, West Conshohocken: pp 8.
- [3] ASTM C1260 (2001): Standard test method for potential alkali reactivity of aggregates (mortar-bar method). American Society for Testing & Materials, ASTM International, West Conshohocken: pp 5.
- [4] ASTM C1293 (2001): Standard test method for determination of length change of concrete due to alkali-silica reaction. American Society for Testing & Materials, ASTM International, West Conshohocken, PA: pp6.
- [5] ASTM C856 (2002): Standard practice for petrographic examination of hardened concrete. American Society for Testing & Materials, ASTM International, West Conshohocken: pp16.
- [6] Kihara, Y (1986) Alkali-aggregate reaction: mineralogical aspects: Proceedings of the First National Symposium on Aggregates, Sao Paulo University, Brazil: 127-138.
- [7] Hobbs, D W (1988): Alkali-silica reaction in concrete. Thomas Telford, London: pp 83.
- [8] Andersen, KT, and Thaulow, N (1989): The application of undulatory extinction angles (UEA) as an indicator of alkali-silica reactivity of concrete aggregates, les réactions liants-granulats dans les bétons. Journées d'étude, École Nationale des Ponts et Chaussées, Paris: 20-21.
- [9] Shayan, A (1993): Alkali-reactivity of deformed granitic rocks: a case study. Cement and Concrete Research (23): 1229-1236.
- [10] Broekmans, MATM (2002): The alkali-silica reaction: mineralogical and geochemical aspects of some Dutch concretes and Norwegian mylonites. PhD-thesis. Utrecht University, The Netherlands. *Geologica Ultraiectina* (217): pp144.
- [11] Rodrigues, EP, Kihara, Y, and Sbrighi, CN (1997): The alkali-aggregate reactivity of granitic and quartzitic rocks: proposal of potential reactivity index. Proceedings of the 1<sup>st</sup> Symposium on Alkali-aggregate Reaction in Concrete Structures, CBGB/FURNAS, Goiânia, Brazil: 151-159.
- [12] Hasparyk, NP (1999): Investigation of mechanisms of alkali-aggregate reaction - effect of rice husk ash and silica fume. MSc Dissertation. Federal University of Goiás, Goiânia, Brazil: pp257.
- [13] Monteiro, PJM, Shomglin, K, Wenk, HR, and Hasparyk, NP (2001): Effect of aggregate deformation on alkali-silica reaction. *ACI Materials Journal* (98): 179-183.
- [14] Hasparyk, NP, Gomides, MJ, Andrade, MAS, Silva, HHAB, and Carasek, H (2005): Laboratory study of concretes containing aggregates with sulphides: Proceedings of 47<sup>th</sup> Concrete Brazilian Conference. Brazilian Concrete Institute (IBRACON), Olinda, Brazil: 822-836.
- [15] Gomides, MJ, Cincotto, MA, Hasparyk, NP, and Carasek, H (2007): Study of aggregates with sulphides in concrete: 12<sup>th</sup> International Congress on the Chemistry of Cement (ICCC 2007). Cement Association of Canada, Montréal, Canada: section ST4, n° PST4.057.
- [16] Hasparyk, NP, Monteiro, PJM, and Carasek, H (2000): Effect of silica fume and rice husk ash on the alkali-silica reaction. *ACI Materials Journal* (97): 486-492.
- [17] Hasparyk, NP (2005): Investigation of concretes affected by alkali-aggregate reaction and advanced characterization of exuded gel. PhD-thesis. Federal University of Rio Grande do Sul, Porto Alegre, Brazil: pp326.
- [18] Hasparyk, NP, Lopes, ANM, Cavalcanti, AJCT, and Silveira, JFA (2004): Expansions due to AAR verified in concrete cores and mortars from several power plants in Brazil. In: Tang, M, and Deng, M (editors): Proceedings of the 12<sup>th</sup> International Conference on Alkali-Aggregate Reaction in Concrete, International Academic Publishers, Beijing, China: 888-897.
- [19] Poole, AB (1992): Introduction to alkali-aggregate reaction in concrete. In: Swamy, RN (editor): The alkali-silica reaction in concrete. 1<sup>st</sup> edition. Blackie and Son Ltd, Glasgow: 1-29.
- [20] Sims, I (1992): Alkali-silica reaction: UK experience. In: Swamy, RN (editor): The alkali-silica reaction in concrete. 1<sup>st</sup> edition. Blackie and Son Ltd., Glasgow/London: 122-183.
- [21] Grattan-Bellew, PE, and Danay, A (1992): Comparison of laboratory and field evaluation of alkali-silica reaction in large dams. Proceedings of the 1<sup>st</sup> International Conference on Concrete Alkali-Aggregate Reactions in Hydroelectric Plants and Dams, Canadian Electrical Association (CEA), Fredericton, Canada: pp23.
- [22] Duncan, DB. (1955): Multiple range and multiple F tests. *Biometrics* (11):1-42.

- [23] Folliard, KJ, Thomas, MDA, and Kurtis, KE (2003): Research, development, and technology. In: Guidelines for the use of lithium to mitigate or prevent alkali-silica reaction (ASR), Turner-Fairbank Highway Research Center. Federal High Way Administration, Report No. FHWA-RD-03-047: pp86.
- [24] Kaneyoshi, A, Uchida, H, and Kano, H (2004): Development of ASR suppressing technology (the AAR/Li method). In: Tang, M, and Deng, M (editors): Proceedings of the 12<sup>th</sup> International Conference on Alkali-Aggregate Reaction in Concrete, Beijing, China: 584-591.



Figure 1a: General view of HPP Furnas.

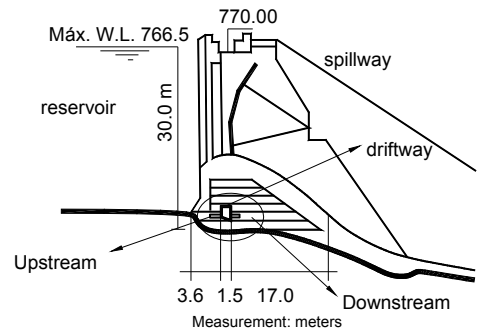


Figure 1b: Sketch showing a cross section of the spillway; detail of the drilling holes (up and downstream directions) in concrete.



Figure 2a: Crack along transversal section of a spillway column



Figure 2b: ASR Gel from cracking in the concrete surface of the spillway driftway.

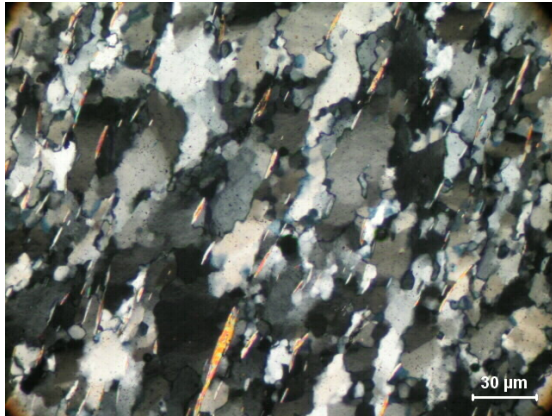


Figure 3: Detail of the quartzite aggregate showing elongated sutured grains of quartz, showing undulatory extinction and fine oriented muscovite (colored) flakes between quartz grains. Optical microscopic image with cross polarized light.

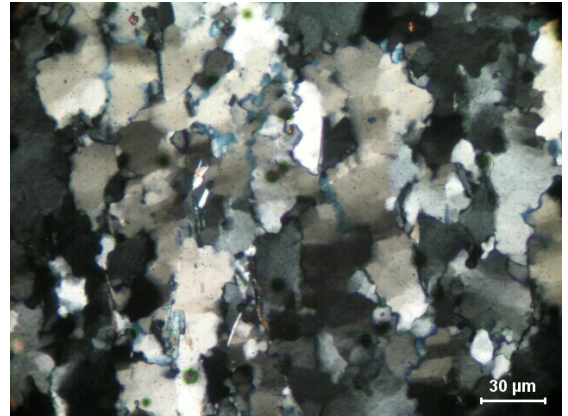


Figure 4: Detail of an area of sutured quartz grains with intense undulatory extinction. Optical microscopic image with cross polarized light.

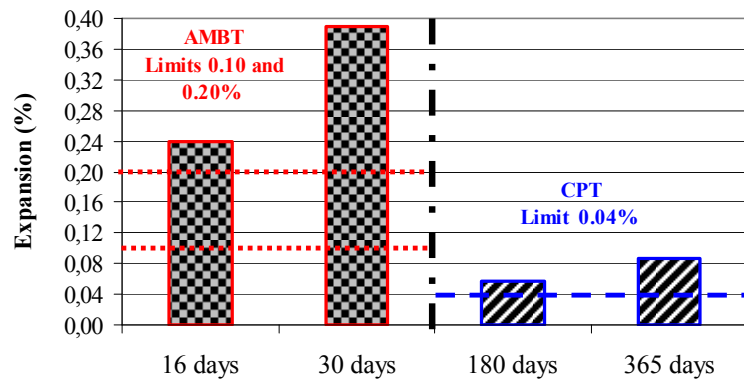


Figure 5: Expansion of mortar bars and concrete prisms



Figure 6: Void filled with white material in the interior and vitreous round the edge (Core 30A-US1).

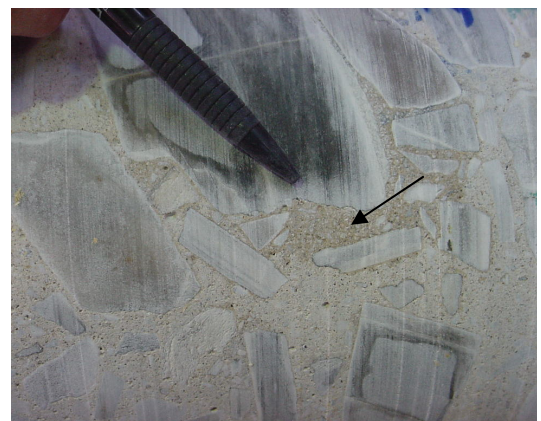


Figure 7: Dark stains in the mortar around aggregates (Core 48A-US1).



Figure 8: Cracks cutting across aggregates and white product filling in the crack (Core 12A-US2).



Figure 9: Dark rim around aggregate (Core 25A-US2).

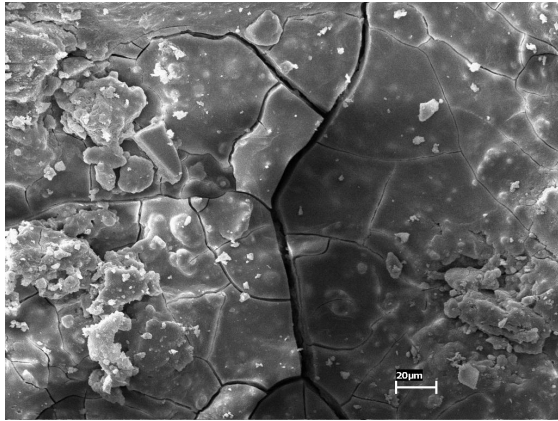


Figure 10: Micrograph of the cracked and botryoidal gel (DS-MI).

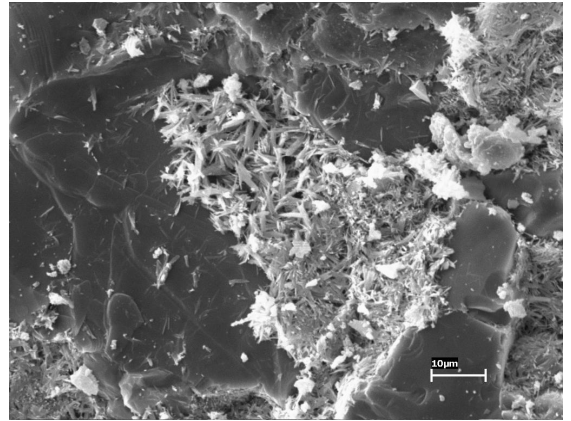


Figure 11: Micrograph of crystallized products on aggregate (DS-MI)

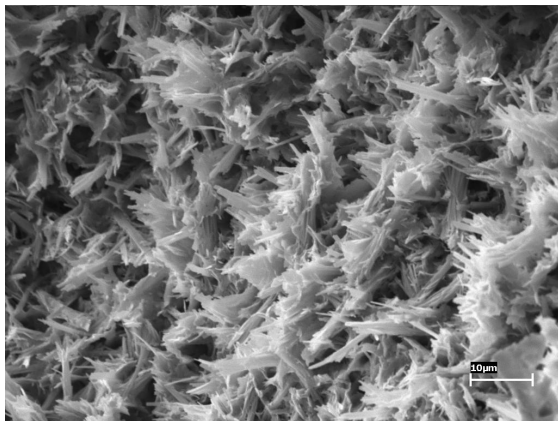


Figure 12: Micrograph of crystallized products inside an air-void (US1-LI)

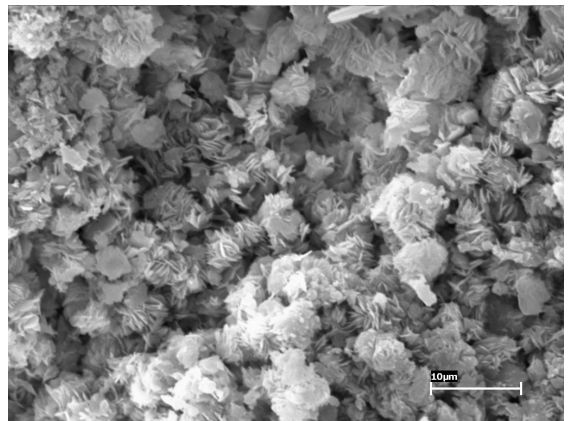


Figure 13: Morphology of the rosette-like reaction products (US1-MI)

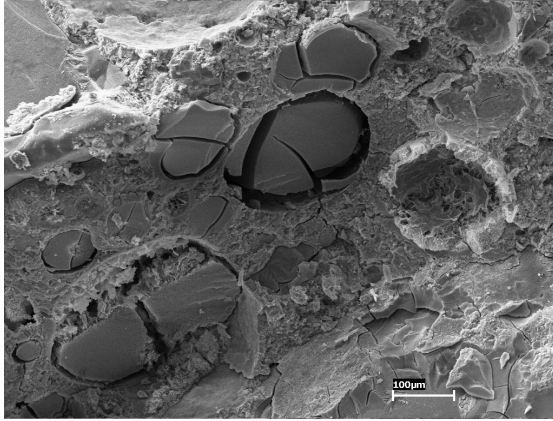


Figure 14: Micrograph showing several voids filled with gel (US2-MI)

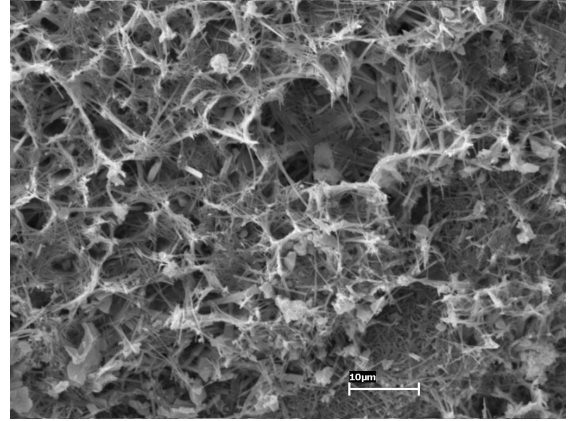


Figure 15: Micrograph indicating laced crystals in the mortar (US2-MI).

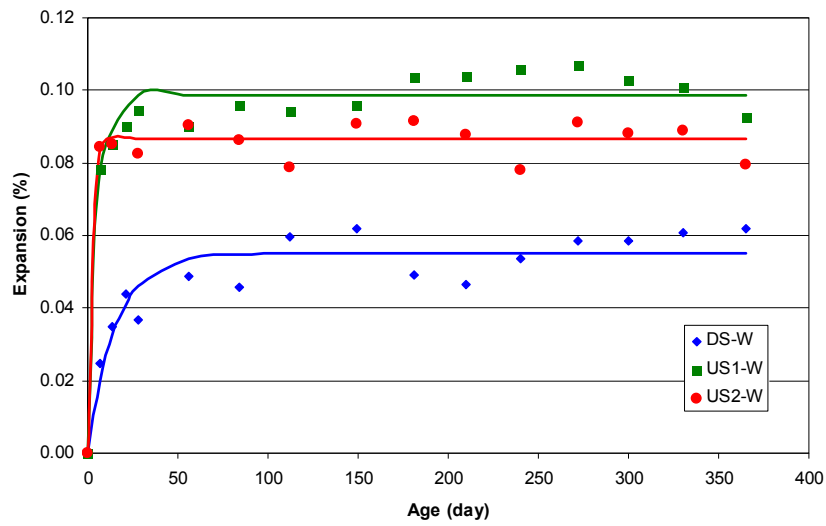


Figure 16: Expansion over time for samples of each class (DS, US1 and US2) immersed in water at 38°C.

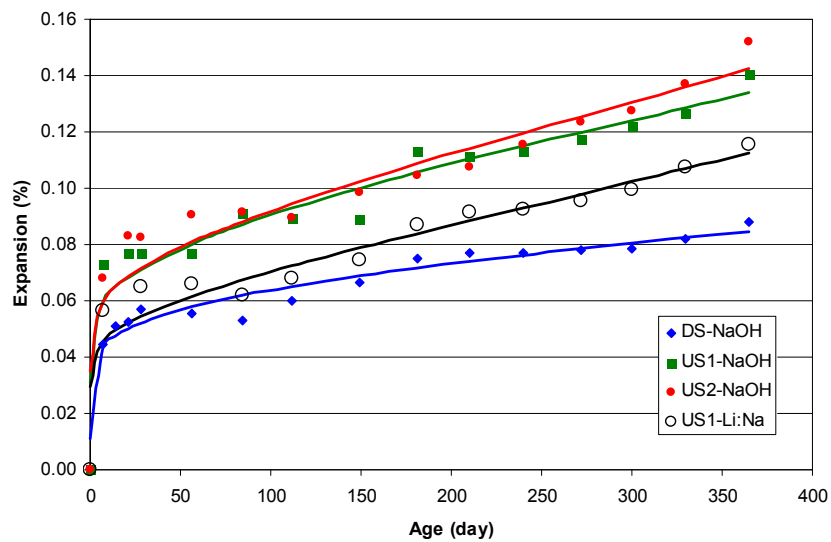


Figure 17: Expansion over time for samples of each class (DS, US1 and US2) immersed in NaOH and LiNO<sub>3</sub>:NaOH solution at 38°C.